RSC Advances

This is an *Accepted Manuscript*, which has been through the Royal Society of Chemistry peer review process and has been accepted for publication.

Accepted Manuscripts are published online shortly after acceptance, before technical editing, formatting and proof reading. Using this free service, authors can make their results available to the community, in citable form, before we publish the edited article. This *Accepted Manuscript* will be replaced by the edited, formatted and paginated article as soon as this is available.

You can find more information about *Accepted Manuscripts* in the Information for Authors.

Please note that technical editing may introduce minor changes to the text and/or graphics, which may alter content. The journal's standard Terms & Conditions and the Ethical guidelines still apply. In no event shall the Royal Society of Chemistry be held responsible for any errors or omissions in this *Accepted Manuscript* or any consequences arising from the use of any information it contains.

ROYAL SOCIETY OF CHEMISTRY

www.rsc.org/advances

RSC Advances

RSCPublishing

ARTICLE

Supercritical fluid processing of nitric acid treated nitrogen doped graphene with enhanced electrochemical supercapacitance

Cite this: DOI: 10.1039/x0xx00000x

Received 00th January 2012,
Accepted 00th January 2012

DOI: 10.1039/x0xx00000x

www.rsc.org/

S. Suresh Balaji and M. Sathish*

Supercritical fluid processing of nitrogen (N) doped graphene and nitric acid treated N-doped graphene are demonstrated using urea as nitrogen source. The qualitative and quantitative information of doped N in the graphene sheets is investigated using Fourier transform infrared spectroscopy, Raman spectroscopy, X-ray diffraction, elemental analysis and X-ray photoelectron spectroscopy analysis. The surface morphology and physical nature of the samples are demonstrated using scanning electron and transmission electron microscopic analysis. The electrochemical performance of prepared electrode materials is characterized using cyclic voltammetry and galvanostatic charge-discharge analysis in a conventional three-electrode system. Nitric acid treated N-doped graphene prepared using supercritical fluid processing shows an enhanced specific capacitance of 261 Fg^{-1} at a current density of 0.5 A/g. In addition, it shows 126 % capacitance retention after 1000 cycles of charge-discharge and it is stable up to 3000 cycles at a current density of 5 A/g.

Introduction

Supercapacitors are indispensable energy storage devices because of their high power performance, long life cycle and low cost.[1] Thus, they have received potential application in devices such as portable electronics, hybrid electric vehicles and so on.[2] However, the use of supercapacitor for above applications is limited by its lower energy density compared to batteries. A major confront in this field is to maximise its energy density and concurrently maintain its high power capability and long cycle life.[1] Based on their charge storage mechanism, supercapacitors can be categorized into two groups namely an electric double-layer capacitor (EDLC) and pseudocapacitor. Carbon based materials are used in EDLC because of their high surface area, good conductivity, light weight etc.[3-5] Redox-active materials such as transition-metal hydroxide/oxides[6,7] and conducting polymers[8] are promising electrode material for pseudocapacitors owing to their faradic reactions. However the poor cycling stability, electrical conductivity and high cost would discourage their applications.[9] Attempts have been made to integrate the EDLC and pseudocapacitive materials to attain supreme specific capacitance with optimum cycle life.[2]

Graphene, a single-atom-thick sheet of hexagonally arrayed sp^2-bonded carbon atoms densely crammed into a two-dimensional honeycomb lattice, has been recently regarded as an emerging applications.[10] Its exclusive morphology, superior electrical conductivity, high theoretical specific surface area, and outstanding structural stability enunciate graphene as attractive and promising candidate for supercapacitors.[11, 12] Nevertheless, the chemically derived graphene habitually experience sheet-to-sheet restacking problem which arise as a result of strong interlayer van der Waals force that results loss of its high specific surface area, restriction in electrolyte penetration and ion accessibility.[13] The electronic and chemical properties of graphene can be tailored by inclusion of heteroatoms such as nitrogen (N) in graphene network. The incorporated nitrogen atoms will contribute to the capacitance by faradic reactions.[15] Thus, there are numerous methods have been reported for the synthesis of nitrogen-doped graphene using various routes[9,11,16-20].

Nitrogen containing organic compounds were reported as nitrogen source for N-doped graphene.[10, 11, 14, 20] To the best of our knowledge, there are only few reports where nitric acid is used to activate the graphene sheets. Ni Xiao et al., synthesized graphene from graphene oxide by thermal treatment with the aid of nitric acid and reported a high specific capacitance of 370 F g^{-1} at a current density of 1 A g^{-1} in alkaline medium. It is higher than that of thermally treated graphene without nitric acid (ca.195 F/g at 1 A/g).[13] In this work, we report the synthesis of N-doped graphene as well as nitric acid treated N-doped graphene using a supercritical heat treatment for electrochemical energy storage application. When the temperature and pressure of water is increased, it becomes less dense due to thermal expansion and beyond 380 °C, the density of water diminishes very quickly. Thus, the dielectric constant of water diminishes with decreasing density due to the breakage of hydrogen bonds. Yet the water remains associated and the association strappingly depends upon pressure and temperature in supercritical environment that essentially persuade the solubility phenomena, the reaction chemistry etc. Thus, the supercritical water function as non-aqueous fluid and dissolves non-polar organic compounds like alkanes, aromatics, etc.[21] Supercritical reactions need very short time compared to other methods, induces homogeneous reaction, simple,

*Functional Materials Division, CSIR-Central Electrochemical Research Institute, Karaikudi- 600036, INDIA

RSC Advances Accepted Manuscript

convenient for the bulk preparation of materials and environment friendly. In addition, the gas-like diffusion with solvent-like properties of supercritical fluid makes the method as unique compared to other methods. Recently, attempts have been made to direct exfoliation of graphene from graphite and functionalization of graphene nanosheets using supercritical ethanol. [22, 23] Also, preparation N-doped graphene was attempted through supercritical acetonitrile and ethanol as solvents.[24,25]

Here we have synthesized supercritical heat-treated graphene oxide (SCHGO), nitrogen-doped graphene oxide (NGO), nitric acid treated nitrogen doped graphene oxide (NA-NGO), reduced supercritical heat-treated graphene oxide (RSCHGO), reduced nitrogen doped graphene oxide (RNGO) and reduced nitric acid treated nitrogen doped graphene oxide (RNA-NGO). All the six materials were characterized using various analytical techniques such as XRD, Raman, FT-IR, CHN analysis and FE-SEM. The electrochemical performances of above materials were scrutinized by cyclic voltammetry, galvanostatic charge/discharge and electrochemical impedance analysis in 1M aqueous sulphuric acid solution. The specific capacitance values of SCHGO, NGO, NA-NGO, RSCHGO, RNGO and RNA-NGO are calculated from the galvanostatic charge/discharge curves at a current density of 0.5 A/g.

Experimental section

Materials

Graphite flakes powder (≤20µm, 99%), Polytetrafluoroethylene (PTFE) ($-CF_2-CF_2-)_n$ were purchased from Sigma-Aldrich, India. Sodium nitrate ($NaNO_3$, 99 wt%), potassium permanganate ($KMnO_4$, 99.5 wt%), hydrogen peroxide (H_2O_2, 30 wt%), hydrazine hydrate (H_6N_2O, 99 wt%) were purchased from E-Merck, India. Sulfuric acid (H_2SO_4, 98 wt%) and nitric acid (HNO_3, 72 wt%) were purchased from Ranbaxy laboratories., Ltd. Urea (CON_2H_4, 98 wt%) was procured from HIMEDIA. All the chemicals and reagents used in our experiments were of analytical grade and were used as received without any further purification. Deionized (DI) water was obtained from MILLIPORE water system.

Preparation of graphene oxide (GO)

GO was synthesized from synthetic graphite flakes using modified Hummer's method.[26] In a typical synthesis, 2 g of graphite and 2 g of $NaNO_3$ was mixed with 100 mL of concentrated H_2SO_4 in a 1000 mL round – bottom flask and stirred for 30 min using magnetic stirring. Then, $KMnO_4$ (12 g) was gradually added with constant stirring and the reaction temperature was maintained at below 5 ˚C using ice water bath. Then, the ice water bath was removed and 160 mL DI water was slowly added with vigorous stirring and the temperature was increased to 90 ˚C. After 30 min stirring, the solution was further diluted by addition of 400 mL of DI water followed by 12 mL of H_2O_2 solution (30%), and the resulting mixture was stirred for 1 h. Then, the solution was filtered and washed with hot DI water for several times until the pH of the solution became ~6. The product was dried under vacuum at 90 ˚C for 5 h. This powdered GO was re-dispersed with known amount of water to make a GO solution.

Supercritical fluid treated graphene oxide (SCHGO)

Graphene oxide solution (20 mL) was ultrasonicated for 30 minutes followed by stirring. Then, the above mixture was loaded into stainless steel reactors of total 35 mL capacity and the reactors were placed into a supercritical reactor at 400 °C and a pressure of 20 ~ 25 MPa (slightly above the supercritical temperature and pressure of water) for 1 h. Then, the reactors are allowed to cool naturally and the precipitate was filtered and washed with water and ethanol, and then dried in an oven at 90 °C for overnight.

Preparation of nitrogen-doped graphene oxide (NGO)

Graphene oxide solution (20 mL) and urea were mixed together at 1:1 weight ratio and loaded into stainless steel reactors of total 35 mL capacity and the reactors were placed into a supercritical reactor at 400 °C for 1 h. The precipitate was dispersed in certain quantity of water and then filtered and washed with water for several times and finally with ethanol and then dried in an oven at 90 °C for overnight.

Preparation of nitric acid treated nitrogen-doped graphene oxide (NA-NGO)

Graphene oxide solution (20 mL), urea (1:1 weight ratio) and 250 µL of conc.HNO_3 were mixed together and loaded into stainless steel reactors of total 35 mL capacity and the reactors were placed into a supercritical reactor at 400 °C for 1 h. The resulting precipitate was dispersed in certain quantity of water and then filtered and washed with water and ethanol. Thus the obtained precipitate was dried in an oven at 90 °C for overnight.

Preparation of hydrazine hydrate treated samples (RSCHGO, RNGO & RNA-NGO)

200 mg of SCHGO or NGO or NA-NGO was dispersed in 30 mL of water and stirred at 90 °C for 1 h. Then, 5 drops of ammonia followed by 5 drops of hydrazine hydrate solutions were added and the resulting mixture was stirred at 90 °C for 3 h. The resulting precipitate was filtered and washed with water for several times and finally with ethanol. The obtained precipitate was dried in an oven at 90 °C for overnight. The reduced samples obtained from SCHGO, NGO and NA-NGO were named as RSCHGO, RNGO and RNA-NGO, respectively.

Materials Characterization

The crystalline nature of the obtained powder materials were examined by powder X-ray diffraction (XRD) measurements using a BRUKER D8 ADVANCE X-ray Diffractometer with Cu K_α radiation (α=1.5418 Å). The 2θ values for the measurement of XRD were 10-70° in steps of 0.02° with a count time of 0.2 s. Fourier transform infrared (FT-IR) spectra were recorded in TENSOR 27 spectrometer (Bruker) using KBr pellet technique from 400 to 4000 cm^{-1}. X-ray photoelectron spectroscopy was measured using Thermo Scientific MULTILAB 2000 base system with X-ray, Auger and ISS attachments containing Twin Anode Mg/Al (300/400 W) X-ray source. The chemical nature and extent of defects in N-doped graphenes were characterized using a laser Raman system (RENISHAW Ivia laser Raman microscope) equipped with a semiconducting laser with a wavelength of 633 nm. CHNS analysis was carried out to estimate the nitrogen content in all the samples by elementar vario EL III. The surface morphology of all the samples were characterized using field-emission scanning electron microscopy (FE-SEM) using Carl Zeiss AG (Supra 55VP) with an acceleration voltage of 5 – 30 kV. The surface area of the RNA-NGO was measured using Quantachrome NOVA 3200e surface area and pore size analyzer. The particle size and dispersion of RNA-NGO was examined using transmission electron microscope (TEM, Tecnai^{TM} G^2 20) working at an accelerating voltage of 200 kV.

Electrochemical Characterization

Electrochemical behaviour of the all the samples were investigated using a conventional three-electrode cell in 1 M H_2SO_4 aqueous solution. The Pt electrode and Ag/AgCl were used as counter electrode and reference electrode, respectively. The working

RSC Advances Accepted Manuscript

electrode was fabricated by mixing 80% weight of sample with 15% weight of carbon AB (conducting carbon) and 5% weight of PTFE (binder) and the resulting paste (3~5 mg) was pressed on stainless steel mesh. Before the electrochemical measurements, the working electrodes were soaked in 1M H_2SO_4 solution for overnight in vacuum desiccators. Cyclic voltammetry and galvanostatic charge–discharge measurements were carried out at different scan rates and different current densities respectively using potentiostat–galvanostat (PG30, AUTOLAB) instrument. Electrochemical impedance spectroscopy (EIS) measurements were carried out in the frequency range of 100 KHz to 1 mHz with an alternate current amplitude of 10 mV.

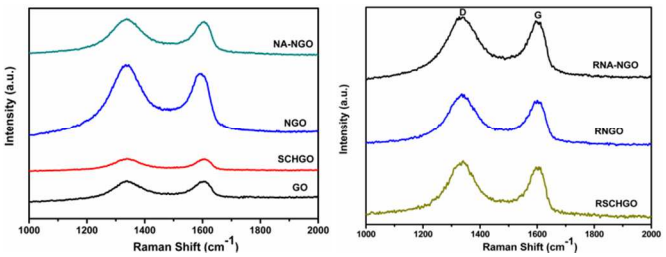

Fig. 1 Raman spectra of GO, SCHGO, NGO, NA-NGO, RSCHGO, RNGO & RNA-NGO.

Results and Discussion

Raman spectroscopy is the most proficient and non-destructive technique to exemplify the structure and quality of carbon materials, principally to evaluate the defects, the ordered and disordered structures and the layers of graphene. In Figure 1, the Raman spectra of electrode materials shows two main peaks centered at around 1340 and 1590 cm^{-1} which were designated as the D band and the G band, respectively.[27] The G band is due to the doubly degenerate E_{2g} phonons at the Brillouin zone and arises from the first-order Raman scattering process.[14] The D band with A_{1g} symmetry is mainly due to the significant defects such as disordered carbon, edge defects, and other defects (sp^3 bonded carbon, dangling bonds, vacancies, and topological defects) in the sp^2 hybridized carbon of the graphitic sheets.[11] The relative intensity ratio of D and G bands (I_D/I_G) can furnish information about the perfection of the graphitic layer structure. It can be clearly seen from the Table 1 that the I_D/I_G ratio of samples treated in supercritical water are higher than GO. Also, the D band intensity of NGO & NA-NGO is slightly higher than SCHGO due to increment in the number of defects by nitrogen doping. When hydrazine hydrate is used to reduce the samples, RSCHGO and RNGO shows slightly higher I_D/I_G value than their counter parts. However, the RNA-NGO shows slightly lesser I_D/I_G value than the NA-NGO, this may be attributed to the residual hydrazine moieties present on the sample surface. The order of I_D/I_G values are as follows RNGO>RSCHGO>NGO>NA-NGO>RNA-NGO> SCHGO.

The presence of N and its amount in the N-doped samples were confirmed using FT-IR spectroscopy (Fig S1) and CHN analysis, respectively. FT-IR spectroscopic analysis confirmed the doping of N in NGO, NA-NGO, RNGO and RNA-NGO samples. The amount of N-doping obtained from the CHN analysis is shown in Table 1. The un-doped samples SCHGO and RSCHGO show 0.03 and 1.49 % of N, the source of N for the latter sample may be the physically or chemically adsorbed hydrazine molecules that were used during the reduction process. Whereas, the N-doped samples NGO, RNGO, NA-NGO and RNA-NGO samples show significant amount of N-doping. However, the amount of N-doping decreased for the RNGO compared to NGO, this may be attributed to removal of N-containing functional group during the reduction by hydrazine hydrate. For the nitric acid treated samples the variation in N-doping before and after the reduction is minimum compared to NGO&RNGO and SCHGO& RSCHGO.

Table 1. Nitrogen content and I_D/I_G values of SCHGO, RSCHGO, NGO, RNGO, NA-NGO & RNA- NGO samples.

Samples	Nitrogen (wt%)	I_D/I_G Value
GO	0.03	1.01
SCHGO	0.03	1.07
RSCHGO	1.49	1.13
NGO	9.35	1.11
RNGO	7.25	1.14
NA-NGO	3.84	1.08
RNA-NGO	4.68	1.06

X-ray photoelectron spectroscopy is an efficient and commonly used technique to evaluate the characteristics of nitrogen species in carbon materials. The XPS survey spectra of RNA-NGO (Figure 2a) exhibit three distinguished peaks at 284.6, 401 and 532.3 eV corresponding to C1s of C, N1s of the doped N, and O1s respectively.[28] Deconvolution of N 1s peak (Figure 2b) clearly shows three peaks at 398.4, 399.8 and 401.2 eV with a relative intensity of 24, 90 and 23 %, respectively. It is known that there are three kinds of N-doping namely pyridinic-N, pyrrolic-N and graphitic-N in graphene nanosheets that can be distinguished using their binding energies.[29] Among the three different types of nitrogen doping, the peak intensity observed for pyrrolic N is comparatively maximum which implies that the N-doping in graphene skeleton are predominantly in the form of pyrrolic nitrogen. While comparing pyrrolic N with pyridinic N, both are oriented in a highly conjugated π- electron system but in former ring N contributes two p electrons to the π- system and in latter ring N contributes a p electron to the π-system.[30] For graphitic N, a C atom in the hexagonal ring is substituted by N. In the deconvoluted C 1s spectrum of RNA-NGO (Figure 2c) three peaks were observed at 284.9, 286.3 and 289 eV due to the three different carbon environments are present in N-doped graphene nanosheets.[31] The peak at 284.9 eV is assigned to graphite-like sp^2 carbon (C1), the high intensity advocate that most of the C atoms in the RNA-NGO are oriented in a conjugated honeycomb lattice. The peak at 286.3 eV (C2) is attributed to binding energy of carbon in C-N environment.[9] The C 1s peak at 289 eV (C3) with low intensity is ascribed to the binding energy of carbonyl carbon.[32] The broad peak centred around 532.3 eV corresponding to O 1s indicates the presence of various oxygen containing functional groups in RNA-NGO (Figure 2d).

RSC Advances Accepted Manuscript

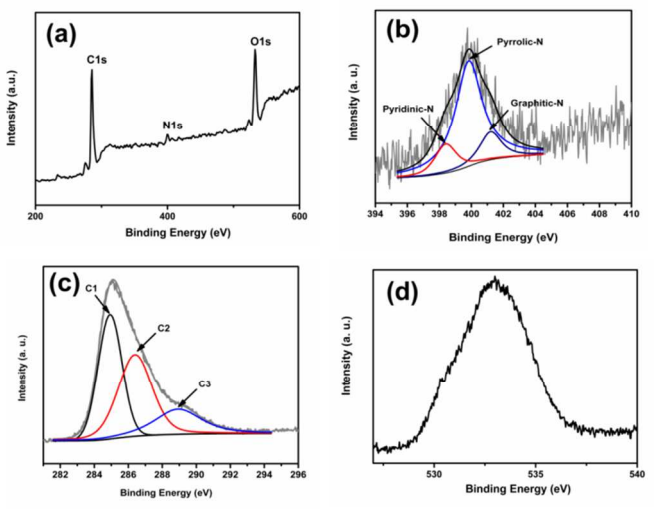

Fig. 2 (a) XPS survey spectrum of RNA-NGO, (b) N1s of RNA-NGO, (c) C1s of RNA-NGO and (d) O 1s of RNA-NGO.

In XRD pattern (Figure 3) a broad diffraction peak around 2θ = 25° and a small peak around 2θ = 44° were observed for SCHGO, NGO, NA-NGO, RSCHGO, RNGO & RNA-NGO samples corresponding to graphite (002) and (100) plane, respectively.[33, 34] Whereas, GO shows a strong peak at 2θ = 10 ~ 12 attributed to (002) plane of GO and the absence of this peak in other samples implied that the complete reduction of graphene oxide during the supercritical water treatment. Thus, it is surmised that instantaneous N-doping in graphene and reduction of graphene oxide can be achieved under supercritical condition in aqueous medium. However, to see the effect of hydrazine reduction, the SCHGO, NGO and NA-NGO samples are further treated with hydrazine solution to obtain RSCHGO, RNGO and RNA-NGO. There was no significant change in the XRD pattern of reduced samples compared to their counterpart.

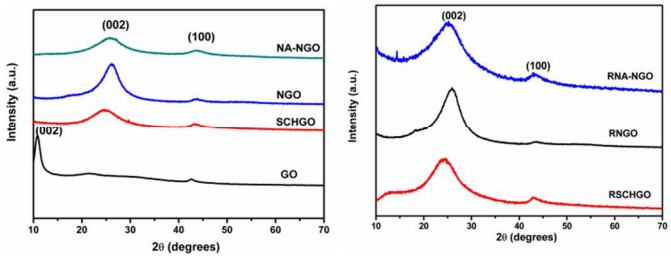

Fig. 3 XRD pattern of GO, SCHGO, NGO, NA-NGO, RSCHGO, RNGO & RNA-NGO.

Figure 4 and 5 demonstrates FE-SEM images of SCHGO, NGO, NA-NGO, RSCHGO, RNGO and RNA-NGO samples. The sheet-like morphology was observed for all the samples except RNA-NGO. The average size of the sheets varies from few nanometres to several microns. The graphene sheets are clearly visible in SCHGO (Figure 4a) whereas the same graphene sheets are scrupulously agglomerated when urea was added in NGO (Figure 4b). Interestingly, the addition of nitric acid along with urea in NA-NGO shows agglomerated thick graphene sheets. The morphology of RSCHGO and RNGO looks like their counter parts SCHGO and NGO, respectively. Whereas, the morphology of RNA-NGO looks thickly crammed graphene nanosheets and it contains more number of macro size pores that enables the electrolyte to penetrate through the entire surface of the electrode materials to facilitate the electrochemical reaction between the electrode-electrolyte interfaces. However, the Brunauer–Emmett–Teller (BET) specific surface area of SCHGO and RNA-NGO were found to be similar as 331 and 323 m^2/g, respectively. The significant difference observed between SCHGO and RNA-NGO in electrochemical performance might be due to more active sites over the RNA-NGO surface which enables the ions in the electrolyte for facilitating the electrode-electrolyte interface.

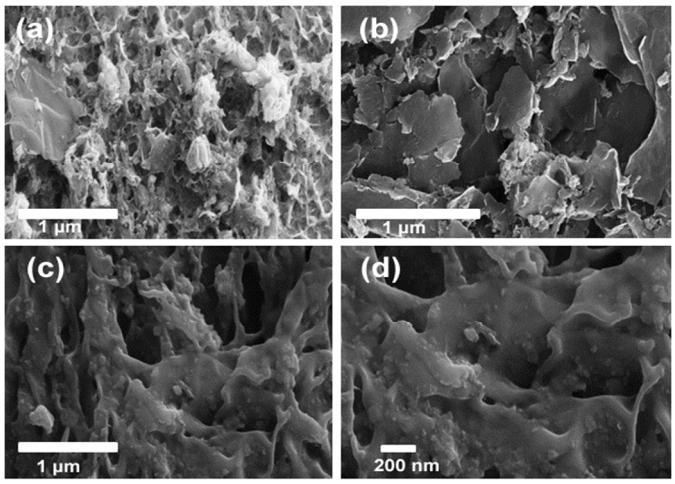

Fig. 4 FE-SEM images of (a) SCHGO, (b) NGO and (c & d) NA-NGO.

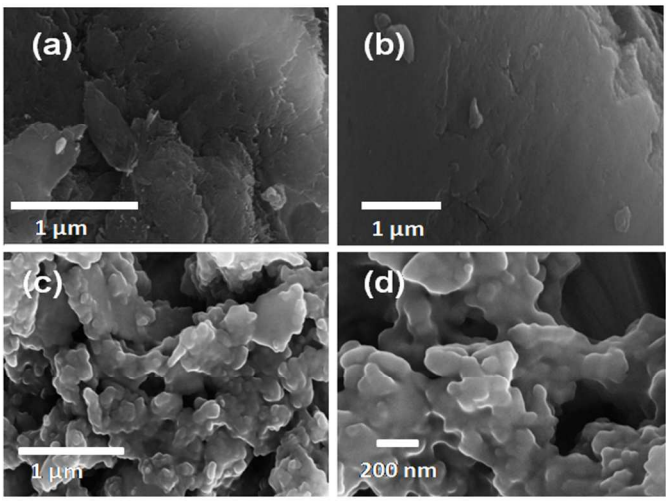

Fig. 5 FE-SEM images of (a) RSCHGO, (b) RNGO and (c & d) RNA-NGO.

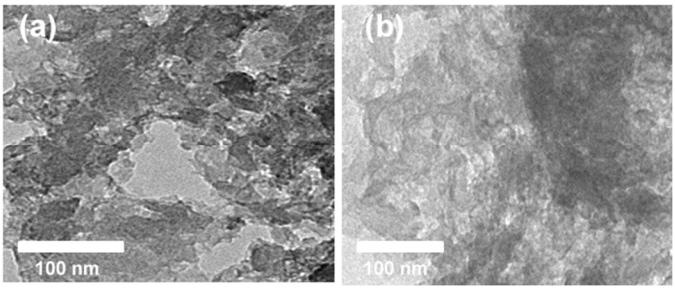

Fig. 6 TEM images of RNA-NGO at different locations.

RSC Advances Accepted Manuscript

The TEM images (Figure 6) of RNA-NGO clearly showed the presence of physically damaged graphene nanosheets with large size pores when compared to GO nanosheets (Fig S2). It is believed that supercritical water treatment of graphene oxide with urea and nitric acid smash up the graphene sheets into graphene nanosheets agglomeration and generates more pores. Consequently, more edge part will be exposed for pseudocapacitor reaction and the addition of urea results N-doping in graphene nanosheets. The above observations are in good agreement with the literature reported nitric acid aided expansion of graphene and generation of pores in graphene.[13]

In order to evaluate the prospective of prepared N-doped graphene as an electrode in supercapacitors, the electrochemical performance of SCHGO, NGO, NA-NGO, RSCHGO, RNGO and RNA-NGO were studied using cyclic voltammetry and galvanostatic charge–discharge in aqueous 1M H_2SO_4 as an electrolyte (Figure 7). The CV profile of SCHGO and RSCHGO mainly revealed the pseudocapacitive-like behaviour (Fig 7 a & b). It is surmised that the supercritical treatment introduces more edge-like or more defects in graphene sheets which are accountable for the appearance of redox peaks in CV profile. When urea was added along with GO, the oxygen containing functional groups are appreciably reduced by urea during the supercritical heat treatment that give rise to more EDLC-like behaviour in cyclic voltammetric profile (NGO and RNGO). Besides, the reduction of oxygen containing functional groups in N-doped graphene/graphene oxide (NGO & RNGO) is well supported by FT-IR spectra. Whereas, when nitric acid was added with urea and GO, the resulting NA-NGO and RNA-NGO materials showed improved current density with slight pseudocapacitive-like behaviour. From the above observations it is comprehensible that the supercritical treatment of GO results more edge-like structures in graphene nanosheets and addition of urea results the N-doping. The observed pseudocapacitive-like behaviour with increased current density compared to other two samples (NGO and SCHGO) authenticate that the addition of nitric acid enhances the electrochemical performance.

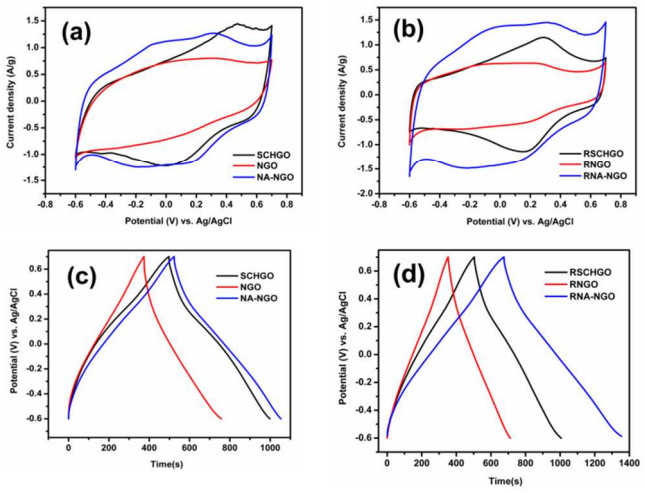

Fig. 7. Cyclic voltammetry curves of (a) SCHGO, NGO & NA-NGO (b) RSCHGO, RNGO & RNA-NGO in aqueous solution of 1M H_2SO_4 at a scan rate of 5 mV/s**.** Galvanostatic charge-discharge behaviour of (c) SCHGO, NGO & NA-NGO and (d) RSCHGO, RNGO & RNA-NGO in aqueous solution of 1M H_2SO_4 at a current density of 0.5 A/g.

Fig 7 c & d shows the galvanostatic charge–discharge curve of all the six samples in a potential window of -0.6 to 0.7 V at a current density of 0.5 A/g. The specific capacitance from the galvanostatic charge/discharge curve was calculated according to the following equation:

$$C_{sp} = \frac{I \times t}{m \times \Delta V}$$

Where C_{sp} is specific capacitance [F g^{-1}], I is galvanostatic discharge current [A], t is the discharge time [s], m is the mass of active material [g], and ΔV is the potential window [V]. The calculated specific capacitance of SCHGO, NGO, NA-NGO, RSCHGO, RNGO and RNA-NGO from galvanostatic charge-discharge curves are 193, 150, 202, 185, 138 and 261 Fg^{-1}, respectively. The pseudocapacitive behaviour in charge/discharge profile is endorsed to the fact that the faradic reaction of electrochemically active hetero atoms and edge-like structure present in the graphene framework. From the charge-discharge profile, it is apparent that the discharge capacity of SCHGO and RSCHGO is relatively higher than those of nitrogen doped NGO and RNGO samples. It is worthy to note here that though the NGO and RNGO have N-doping, the electrochemical resistance is much higher than SCHGO and RSCHGO (Fig S3 & Table S1). Similarly, the RNA-NGO showed higher specific capacitance and low resistance than the RSCHGO and RNGO. This clearly indicates that in-addition to N-doping, the electrochemical resistance has played vital role on specific capacitance. The nitric acid treatment during the supercritical treatment enables moderate N-doping with low electro chemical resistance (3.71Ω, Fig S3 & Table S1). Thus, the specific capacitance of RNA-NGO is higher than all other samples.

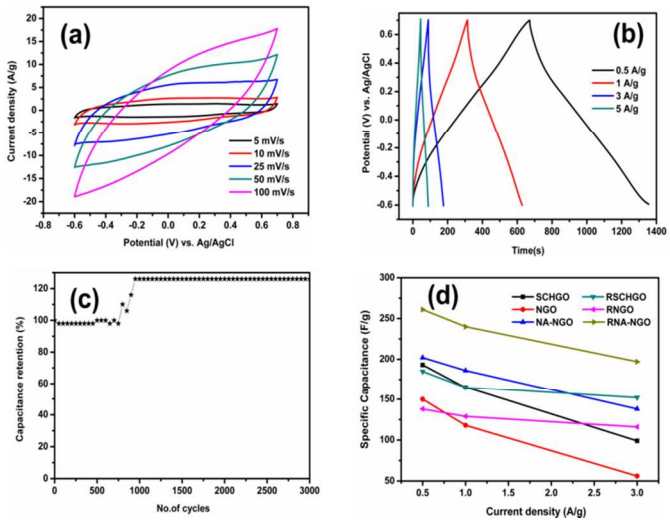

Fig. 8. (a) Cyclic voltammetric curve of RNA-NGO at different scan rates. (b) galvanostatic charge-discharge profile of RNA-NGO at different current rates (c) cycle performance of RNA-NGO at 5 A/g current rate & (d) plot of specific capacitance against current density of SCHGO, NGO, NA-NGO, RSCHGO, RNGO and RNA-NGO in aqueous of 1M H_2SO_4 solution.

Cyclic voltammetric profile of RNA-NGO at different scan rates is shown in Figure 8a and it clearly indicates the EDLC behaviour. Figure 8b demonstrates the galvanostatic charge-discharge profile of RNA-NGO at different current rates and it indicates when the current density enhances the discharge period decreases proportionately. In order to scrutinize cycling stability of RNA-NGO, galvanostatic charge-discharge experiment was carried out for 3000 cycles at a current density of 5 A/g (Figure 8c). The above electrode shows 98% capacitance retention up to 750 cycles

RSC Advances Accepted Manuscript

and after that the specific capacitance was slightly increases, at the end of 3000th cycle an augmented specific capacitance of 213 Fg^{-1} (126 %) was observed. This is attributed to the cycling-induced improvement in surface wetting of the electrode materials that leads to more electro-active surface areas. Similar phenomena have also been reported.[36] Figure 8d shows the specific capacitance of all the six electrode materials at different current densities. The RNA-NGO shows a specific capacitance of 197 F/g at a high current density of 3 A/g. Thus, the RNA-NGO is promising electrode materials for electrochemical supercapacitor applications.

Conclusions

Supercritical fluid processing of N-doped graphene and nitric acid treated N-doped graphene were synthesized using graphene oxide and urea. I_D/I_G values from Raman spectra and XRD pattern analysis indicated the formation of highly defect containing N-doped graphene nanosheets under supercritical water treatment. FT-IR spectra analysis substantiates the existence of nitrogen in graphene framework and CHN analysis revealed the amount of N content in N-doped samples. The N1s binding values obtained from the XPS spectrum of RNA-NGO sample validate the existence of nitrogen in graphene as pyrrolic-N, pyridinic-N and graphitic-N form. The addition of nitric acid significantly alters the amount and nature of N doping in graphene sheets. Among the supercritical water treated un-doped, doped and nitric acid treated N-doped samples, the RNA-NGO exhibited the good capacitive behaviour and attained a maximum specific capacitance value of 261 F/g at a current density of 0.5 A/g in aqueous solution of 1 M H_2SO_4. Due to cycling-induced improvement in surface wetting a 126% specific capacitance retention was observed for RNA-NGO electrodes upto 3000 cycles charge-discharge at 5 A/g current density.

Acknowledgements

We thank CSIR, India for financial support through MULTIFUN (CSC0101) project.

Notes and references

1 B. You, L. Wang, L. Yao, J. Yang, *Chem. Commun*., 2013, **49**, 5016.
2 P. Simon, Y. Gogotsi, *Nat. Mater*., 2008, **7**, 845.
3 M. Zhi, C. Xiang, J. Li, M. Li, N. Wu, *Nanoscale*, 2013, **5**, 72.
4 L. L. Zhang, R. Zhou, X. S. Zhao, *J. Mater. Chem*., 2010, **20**, 5983.
5 L. Deng, R. J. Young, I. A. Kinloch, A. M. Abdelkader, S. M. Holmes, D. A. De Haro-DelRio, S. J. Eichhorn, *ACS Appl. Mater. Interfaces*, 2013, **5**, 9983.
6 X. Zhao, B. M. Sánchez, P. J. Dobson and P. S. Grant, *Nanoscale*, 2011, **3**, 839
7 R. B. Rakhi, W. Chen, D. Cha, H. N. Alshareef, *J. Mater. Chem*., 2011, **21**, 16197.
8 M. Sathish, S. Mitani, T. Tomai, I. Honma, *J. Mater. Chem*., 2011, **21**, 16216.
9 H. Gómez, M. K.Ram, F. Alvi, P. Villalba, E. (Lee) Stefanakos, A. Kumar, *J. Power Sources*, 2011, **196**, 4102.
10 Y. Chang, G. Han, J. Yuan, D. Fu, F. Liu, S. Li, *J. Power Sources*,2013, **238**, 492.
11 B. Zheng, T.-W. Chen, F.-N. Xiao, W.-J. Bao, X.-H. Xia, *J. Solid State Electrochem*., 2013, **17**, 1809.
12 L. Jiang and Z. Fan, Nanoscale, 2014, **6**, 1922.
13 N. Xiao, H. Tan, J. Zhu, L. Tan, X. Rui, X. Dong, Q. Yan, *ACS Appl. Mater. Interfaces*, 2013, **5**, 9656.
14 H. Wang, T. Maiyalagan, X. Wang, *ACS Catal*., 2012, **2**, 781.
15 M. Zhou, X. Li, J. Cui, T. Liu, T. Cai, H. Zhang, S. Guan *Int. J. Electrochem. Sci.,* 2012*,* **7**, 9984.
16 X. Li, H. Wang, J.T. Robinson, H. Sanchez, G. Diankov, H. Dai, *J. Am. Chem. Soc*., 2009, **131**, 15939.
17 D. Wei, Y. Liu, Y. Wang, H. Zhang, L. Huang, G. Yu, *Nano Lett*., 2009, **9**, 1752.
18 T. K. Shruthi, N. Ilayaraja, D. Jeyakumar, M. Sathish, *RSC Adv*., 2014, **4**, 24248.
19 D. Long, W. Li, L. Ling, J. Miyawaki, I. Mochida, S.-H. Yoon, *Langmuir*, 2010, **26**, 16096.
20 H. Sun, Y. Wang, S. Liu, L. Ge, L. Wang, Z. Zhu, S. Wang, *Chem. Commun*., 2013, **49**, 9914.
21 J. Duan, Y. Shim, H. J. Kim, *J. Chem. Phys*., 2006, **124**, 204504.
22 D. Rangappa, K. Sone, M. Wang, U. K. Gautam, D.Golberg, H.Itoh, M. Ichihara, I. Honma, Chem. Eur. J. 2010, **16**, 6488
23 J. H. Jang, D. Rangappa, Y. U. Kwon, I. Honma, *J. Mater. Chem.*, 2011, **21**, 3462.
24 W. Qian, X. Cui, R. Hao, Y. Hou, Z. Zhang, *ACS Appl. Mater. Interfaces*, 2011, **3**, 2259.
25 M. Sathish, S. Mitani, T. Tomai, I. Honma, *J. Mater. Chem*. A, 2014, **2**, 4731
26 W. S. Hummers, R. E. Offeman, *J. Am. Chem. Soc*, 1958, **80**, 1939.
27 Z. Jin, J. Yao, C. Kittrell, J. M. Tour, *ACS Nano*, 2011, **5**, 4112.
28 X. Du, C. Zhou, H.-Y. Liu, Y.-W. Mai, G. Wang, *J. Power Sources*, 2013, **241**, 460.
29 K. Gopalakrishnan, K. Moses, A. Govindaraj, C.N.R. Rao, *Solid State Commun*., 2013, **175-176**, 43.
30 D. Deng, X. Pan, L. Yu, Y. Cui, Y. Jiang, J. Qi, W.-X. Li, Q. Fu, X. Ma, Q. Xue, G. Sun, X. Bao, *Chem. Mater*., 2011, **23**, 1188.
31 Y. Lu, F. Zhang, T. Zhang, K. Leng, L. Zhang, X. Yang, Y. Ma, Y. Huang, M. Zhang, Y. Chen, *Carbon*, 2013, **63**, 508.
32 C. Zhang, L. Fu, N. Liu, M. Liu, Y. Wang, Z. Liu, *Adv. Mater*., 2011, **23** , 1020.
33 Z. Lin, G. H. Waller, Y. Liu, M. Liu, C. Wong, *Nano Energy*, 2013, **2**, 241.
34 M.-Y. Yen, C.-K. Hsieh, C.-C. Teng, M.-C. Hsiao, P.-I. Liu, C.-C.M. Ma, M.-C. Tsai, C.-H. Tsai, Y.-R. Lin, T.-Y. Chou, *RSC Adv*., 2012, **2**, 2725.
35 Y. Gamo, A. Nagashima, M. Wakabayashi, M. Terai, C. Oshima, *Surf. Sci*., 1997, **374**, 61.
36 T.-Y. Wei, C.-H. Chen, H.-C. Chien, S.-Y. Lu, C.-C. Hu, *Adv. Mater*., 2010, **22**, 347.

RSC Advances Accepted Manuscript

Graphical abstract:-

Supercritical fluid processing of nitric acid treated nitrogen doped graphene with enhanced electrochemical supercapacitance

*S. Suresh Balaji and M. Sathish**

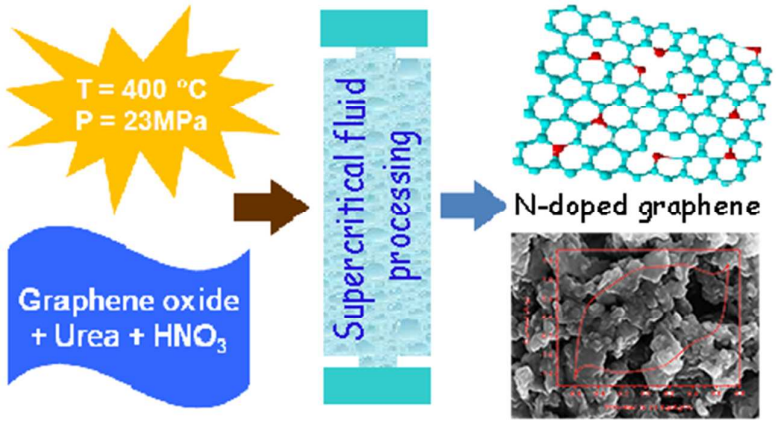

Supercritical fluid assisted synthesis of N-doped graphene as well as nitric acid treated in-situ N-doped graphene were demonstrated using urea as nitrogen source. Nitric acid treated RNA-NGO showed a maximum specific capacitance of 261 Fg^{-1} at 0.5 A/g. Cycling-induced surface wetting results 126% specific capacitance retention after 1000 cycles charge-discharge at 5 A/g.

RSC Advances Accepted Manuscript